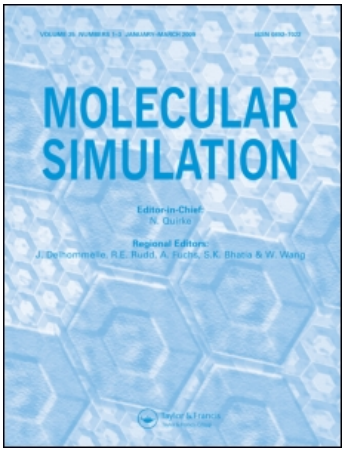

Molecular Simulation
Publication details, including instructions for authors and subscription information:
http://www.informaworld.com/smpp/title~content=t713644482

Numerical Integration of Equations of Motion with a Self-Consistent Field given by an Implicit Equation

Jiří Kolafa[ab]
[a] Lindø center for Applied Mathematics, Odense University, Odense, Denmark [b] Department of Chemistry, Northwestern University, Illinois, U.S.A.

To cite this Article Kolafa, Jiří(1996) 'Numerical Integration of Equations of Motion with a Self-Consistent Field given by an Implicit Equation', Molecular Simulation, 18: 3, 193 — 212
To link to this Article: DOI: 10.1080/08927029608024123
URL: http://dx.doi.org/10.1080/08927029608024123

Molecular Simulation, 1996, Vol. 18, pp. 193–212
Reprints available directly from the publisher
Photocopying permitted by license only

NUMERICAL INTEGRATION OF EQUATIONS OF MOTION WITH A SELF-CONSISTENT FIELD GIVEN BY AN IMPLICIT EQUATION

JIŘÍ KOLAFA[1]

Lindφ center for Applied Mathematics, Odense University,
Forskerparken 10, 5230 Odense M, Denmark
and
Northwestern University, Department of Chemistry,
2145 Sheridan Road, Illinois 60203-3113, U.S.A.

(Received May 1996; accepted June 1996)

Numerical integration methods for equations of motion with the right hand side containing an implicit equation (*e.g.* an equation for the self-consistent electrostatic field in the system of polarizable molecules) are studied. Stable second-order predictors suitable for the Verlet (leap-frog) integrator and allowing one evaluation of the forces per integration step are proposed. Different strategies making the use of only partly stable higher-order predictors possible are discussed.

Keywords: Predictor-corrector; self-consistent field; molecular dynamics

1. INTRODUCTION

An accurate description of properties as the dielectric constant or solvation of ions by molecular simulation calculations requires an accurate model of the electrostatic force field. It should generally include the effect of polarizability where the electrostatic field changes charge distribution in molecules which again change the electrostatic field so that an implicit equation has to be solved to obtained the self-consistent field. Such a force field is no longer pairwise additive.

---

[1]On leave of absence from E. Hála Laboratory of Thermodynamics, Institute of Chemical Process Fundamentals, Acad. Sci., 165 02 Prague 6-Suchdol, Czech Republic

First works in this field proceeded directly according to the definition of polarizability [1, 2, 3]: Point-dipoles are added to the polarizable atoms and their values are determined from the electrostatic field acting on them. The field is recalculated with the new values of induced dipoles and procedure is repeated until a sufficiently accurate self-consistent field is obtained. Alternatively, it is possible to mimic the point dipoles by redistributing existing partial charges in the molecule or adding auxiliary point charges [4], but the equations for the self-consistent field are still solved by iterations.

One way to avoid expensive interations is to predict the field on the basis of its knowledge from previous integration steps [5, 6]. This method with the simplest predictor of Gear type (equivalent to the Taylor expansion or Newton interpolation formula) improves efficiency, but the iteration procedure is not completely avoided.

A different approach, called Lagrangian method [7, 8], uses Gaussian distribution of additional charges which are treated as dynamic variables. If motions associated with these additional degrees of freedom are much faster than other motions in the system, the electrostatic field of the additional charges follows changes in the systems and represents a good approximation of the self-consistent field.

In this paper we do not assume any particular method for representing the induced dipoles and some of the results apply to the time development of any dynamic quantity given by an implicit equation in the self-consistent form $x = f(x, t)$. We will try to reduce the number of iterations of the self-consistent field per step to a minimum, *i.e.* one, by predicting the field using generalized predictors optimized to reach the maximum stability of the predictor-corrector procedure. This goal is achieved without any additional assumptions on the rate of convergence only for the second-order predictor suitable for the popular Verlet (leap-frog) method of integration of the equations of motion and its variations.

Using a fixed number of iterations per step also means that the self-consistent field predictor is embedded to the integrator of the equations of motions. The accuracy of the field is thus consistent with the accuracy of the integrator and no *a priori* accuracy limit is needed for the iterations.

In Section 2 of this paper we, after recalling basic relationships, propose a model for studying stability of predictors for implicit equations. Particular second, third and fourth order predictors derived in Section 3 are tested in Section 4 by simulations on a realistic system. Simulation details are postponed to the Appendix.

2. THEORY

2.1. Basic Relationships

Let D denote a set of n variables describing our dynamic system. For instance, for N polarizable point-dipoles $\mathbf{D}_i$ (3D vectors) one may write $D=(\mathbf{D}_1,\ldots,\mathbf{D}_N)$ and $n=3N$. The implicit equation for the self-consistent field takes the form

$$D = F(D) \tag{1}$$

where, for notation simplicity, any dependence on other degrees of freedom (positions of other charges and permanent dipoles in the system) as well as explicit time dependence are omitted.

As written, (1) represents a recipe to calculate the field by iterations. By linearizing it,

$$\Delta D_i = \sum_{j=1}^{n} \left(\frac{\partial F_i}{\partial D_j}\right) \Delta D_j \equiv \sum_{j=1}^{n} M_{ij} \Delta D_j \tag{2}$$

where $\Delta D = D - D^0$ and D^0 is the solution of (1), we see that the iterations converge from a point close enough to the solution if the largest eigenvalue λ of matrix M is, in the absolute value, less than unity. This must be satisfied for any physically well-defined system.

By writing the dipole-dipole interactions directly [2] (operator F is already linear in this case) it can be shown that matrix M is symmetric and thus all its eigenvalues are real. Though this is our main interest, we will touch the case of general implicit equation (1) with possibly complex eigenvalues of M as well.

By introducing the mixing iteration parameter (relaxation parameter) ω, equation (1) can be rewritten to the form

$$D = \omega F(D) + (1-\omega)D \tag{3}$$

Let us assume that the values of vectors D in a certain number of previous simulation steps at times, $t, t-h, t-2h, \ldots$, where h denotes the timestep, are recorded. (Alternatively, this history can be represented by the vector of time derivatives $D(t), h\dot{D}(t), (h^2/2)\ddot{D}(t)\ldots$[9, 10].) A general m-order predictor

using $m+k$ last values can be written by

$$D^p(t+h) = \sum_{i=0}^{m-1} \binom{m}{i+1} (-1)^i D(t-ih) + \sum_{j=1}^{k} A_j \sum_{i=0}^{m} \binom{m}{i} (-1)^i D(t-[i+j-1]h) \tag{4}$$

This predictor has a local (one step) error of $O(h^m)$. The simplest case $k=0$ is identical to the predictor used in the m-value Gear predictor-corrector method.

2.2. Stability

Stability means that errors (caused by higher order terms than those taken into account by the predictor along with rounding, cutoff and other errors) do not cumulate during the predictor-corrector procedure but decrease as fast as possible.

The coefficients at terms $D(t-ih)$ in predictor (4) are alternating and increasing for larger m which means that the stability properties of higher-order predictors are poor. The reason for additional ($k \neq 0$) terms in (4) is just to have more degrees of freedom to improve the stability.

Stability of integrators for ordinary differential equations of order n is studied by means of homogeneous equation $y^{(n)} = \lambda y$ [10, 11]. Analogously, we will use predictor (4) to solve equation (1) for the following 'primitive' right-hand side

$$F(D) = \lambda D \tag{5}$$

where now D is a scalar and λ, $|\lambda| < 1$, represents the highest eigenvalue of matrix M. While λ can be eliminated from differential equations by a time transformation, the same trick cannot be applied to 'zero order differential equation' (5) and the whole range of possible λ must be taken into account.

We want to evaluate the right-hand side F only once in each step. Using the mixing iteration parameter ω we thus write the corrector as

$$D(t+h) = \omega F(D^p(t+h)) + (1-\omega) D^p(t+h) \tag{6}$$

which along with (4) defines the recurrence for error propagation. The characteristic equation of this recurrence is

$$\zeta^{m+k} = \lambda_\omega \sum_{l=1}^{m+k} C_l \zeta^{m+k-l} \tag{7}$$

where

$$C_l = \binom{m}{l}(-1)^{l+1} + \sum_{j=\max\{0,l-k\}}^{l-1} \binom{m}{j}(-1)^j A_{l-j} \tag{8}$$

and

$$\lambda_\omega = \lambda\omega + (1-\omega) \tag{9}$$

The convergence or divergence of the predictor is linear with the quotient given by the maximum (in the absolute value) root $\xi_{\max}$ of equation (7). The condition of stability is thus $|\xi_{\max}| < 1$. Note that for $\lambda = 0$ and $\omega = 1$ (right-hand side is given explicitly) we have $\xi_{\max} = 0$ and the solution $D = 0$ is reached within a finite number of steps, namely $m + k$.

2.3. Time Reversibility

In the previous paragraph we have studied how fast random inaccuracies decay during the predictor-corrector procedure. Here we will study the systematic errors caused by terms of higher order than the predictor. The 'primitive' right-hand side will be now

$$F(D) = \lambda D + (1-\lambda) f(t) \tag{10}$$

where $f(t)$ is a certain function continuous with a sufficient number of derivatives and $t = nh$. After inserting the Taylor expansion of $f(t)$ into (4) and (10) we get the first two error terms

$$D(t) - f(t) = \frac{\lambda}{1-\lambda}[E_m f^{(m)}(t)\, h^m + E_{m+1} f^{(m+1)}(t) h^{m+1} + \cdots] \tag{11}$$

where

$$E_m = \sum_{j=1}^{k} A_j - 1 \tag{12}$$

$$E_{m+1} = \frac{m}{2} - \sum_{j=1}^{k} \left(\frac{m}{2} + j\right) A_j \tag{13}$$

If the order m is odd number, the first error term changes its sign by transformation $t \to -t$ and is thus time-irreversible. If, for instance,

$f(t) = \cos(t)$ (harmonic oscillator), $D(t)$ will have a phase error, leading to a systematic energy drift in molecular dynamics simulations. This term cannot be removed by any other method than by fulfilling $\sum_{j=1}^{k} A_j = 1$ which is equivalent to increasing the order of the predictor.

If, on the other hand, m is even number, the first error term does not depend on the direction of time. The approximation $D(t)$ for the harmonic oscillator will have an amplitude error of order h^m but the phase error of order h^{m+1} and energy will be conserved with higher precision. If it even happens to choose such A_j so that E_{m+1} vanishes, the next time-irreversible term will have the order as high as h^{m+3}.

2.4. Convergence of Iterations and Optimizing the Predictors

The stability of predictors depends on the value of λ representing the rate of convergence of the self-consistent field iterations. An ideal predictor should be stable in the whole physically acceptable range $\lambda \in (-1, 1)$. Unfortunately, this cannot be achieved for higher order predictors. We would therefore like to estimate the range of eigenvalues of matrix M, $(\lambda_{\min}, \lambda_{\max}) \subset (-1, 1)$, and to make use of this knowledge in optimizing predictors.

The range $(\lambda_{\min}, \lambda_{\max})$ for a general polarizable system may be difficult to predict. A pair of identical polarizable atoms has a pair of eigenvalues of opposite signs and it holds $|\lambda_{\min}| = |\lambda_{\max}|$. This degeneration is a direct consequence of pairwise nature of the forces: In one step particle A induces a dipole on particle B and in the second step it is back influenced by this induced dipole. Numerical calculations give for three and four atoms in a line $|\lambda_{\min}| < \lambda_{\max}$, while more compact configurations as three atoms in a triangular arrangement, atoms at vertices of a square, regular tetrahedron or a regular hexagon have $|\lambda_{\min}| > \lambda_{\max} > 0$. Our experience shows that the latter case is typical for complex realistic systems.

The values of minimum and maximum eigenvalues of matrix M are available experimentally by calculating a series of iterations $D^{(j)}$, $j = 0, 1, \ldots$, from equation (3), starting *e.g.* from a random initial configuration $D^{(0)}$. The estimate of $\lambda_{\min,\omega}$ (and analogously $\lambda_{\max,\omega}$) is given by

$$\lambda_{\min,\omega} = \min_{i=1}^{N} \lim_{j \to \infty} [D_i^{(j+1)} / D_i^{(j)}] \tag{14}$$

provided that the limit exists. The value of $\lambda_{\min} \equiv \lambda_{\min,1}$ and $\lambda_{\max}$ are then obtained by inverting equation (9),

$$\lambda = [\lambda_\omega - (1 - \omega)]/\omega \tag{15}$$

In typical cases $|\lambda_{\min}| > \lambda_{\max}$ and the calculations with $\omega = 1$ give directly $\lambda_{\min} < 0$ while certain $\omega < 1$ will give $\lambda_{\max,\omega}$.

The fastest convergence of iterations (3) (without any prediction) can be expected if condition $\lambda_{\min,\omega} = -\lambda_{\max,\omega}$ is satisfied, *i.e.* for

$$\omega = 2/(2 - \lambda_{\min} - \lambda_{\max}) \tag{16}$$

The above condition is to be replaced by the condition for the maximum roots of the characteristic equation

$$|\xi_{\max}(\lambda_{\min}, \omega)| = |\xi_{\max}(\lambda_{\max}, \omega)| \tag{17}$$

to obtain the largest stability of a predictor. (We assume that, for given ω, the maxima of roots $|\xi_{\max}|$ are reached at the end points of interval $\langle \lambda_{\min}, \lambda_{\max} \rangle$, which generally need not be true.)

3. PREDICTORS

In this section we apply the theoretical findings of the previous section and derive practically useful second, third and fourth-order predictors.

3.1. Second-Order Predictors

The second-order predictors are given by (4) with $m = 2$. We will consider only one additional term in equation (4), $k = 1$, because we have found this sufficient. The second-order predictor thus reads as

$$D^p(t + h) = (2 + A_1) D(t) - (1 + 2A_1) D(t - h) + A_1 D(t - 2h) \tag{18}$$

Its characteristic equation (7) is cubic,

$$\xi^3 = \lambda_\omega [(2 + A_1)\xi^2 - (1 + 2A_1)\xi + A_1] \tag{19}$$

Our task is to find such pairs (A_1, ω) so that all roots of (19) are in the absolute value less than unity for all possible real λ from a given range or, if we do not have any knowledge of the system, from the full range $|\lambda| < 1$.

Figure 1 shows the rate of convergence approximated by the maximum (in absolute value) root $|\xi_{\max}|$ in dependence on A_1 and (real) λ for $\omega = 1$ (direct iterations). It is seen that only for $A_1 = -1/2$ the predictor is stable

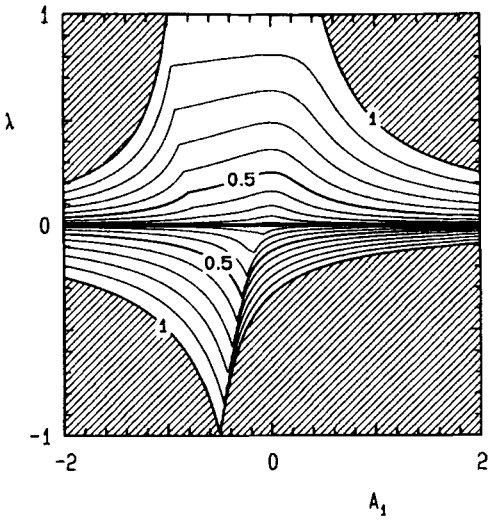

FIGURE 1 The rate of convergence $|\xi_{max}|$ as the function of A_1 and λ for second-order predictor (18) with $\omega = 1$ (direct iteractions). The isoclines go from 0 to 1 by 0.1. The unstable area is shaded.

in the whole physically possible range $|\lambda| < 1$. The simple predictor with $A_1 = 0$ has the range of stability $\lambda \in (-1/3, 1)$.

Since using $\omega < 1$ enlarges the region of stability $(\lambda_{min,\omega}, \lambda_{max,\omega})$ keeping $\lambda_{max,\omega} = 1$ as the fixed point, it follows from Figure 1 that for $-1 \leqslant A_1 \leqslant 1/2$ there exists such ω that the range of stability covers the whole range of $-1 < \lambda < 1$ and that (17) is satisfied. After carrying out some algebra we get the following family of optimized predictors

$$\omega = (2A_1 - 1)/(4A_1) \quad \text{for } -1 \leqslant A_1 \leqslant -1/2 \tag{20}$$

$$= (2A_1 + 2)/(4A_1 + 3) \quad \text{for } -1/2 \leqslant A_1 \leqslant 1/2$$

The predictor for $A_1 = 1/2$ has the best time reversibility (smallest energy drift) because the h^3 error term vanishes (see (11) and (13)).

To provide a deeper insight into the structure of predictors for general implicit equation we show in Figure 2 the rate of convergence $|\xi_{max}|$ as the function of complex λ for several predictors (20). None of them is stable in the whole $|\lambda| < 1$ circle in the complex plane.

If we turn back to the usual real values of λ we can see from Figure 2 that only the already mentioned predictor $(A_1 = -1/2, \omega = 1)$ works uniformly

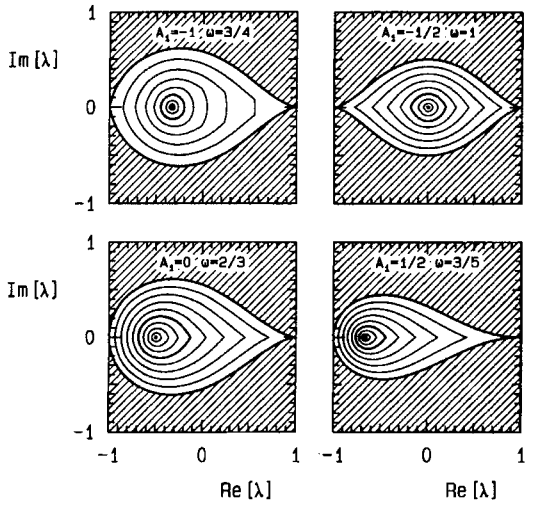

FIGURE 2 The rate of convergence $|\xi_{max}|$ as the function of complex λ for several stable second-order predictor (20). The isoclines go from 0 to 1 by 0.1. The unstable area is shaded.

well for both positive and negative λ. As soon as $A_1 \neq -1/2$, the predictor is expected to work better for negative λ (which need not be disadvantage because this situation is quite typical for realistic polar systems). From two predictors of the same stability the one with higher A_1 should be used because it has lower error coefficient (note that for $A_1 = 1$ we have a third-order predictor which is only partly stable).

The second order predictors are suitable for the Verlet integration method and its variations (three-value Gear method for the 2nd order differential equation). The main advantage of these methods, time-reversibility, is best reproduced by the predictor with $A_1 = 1/2$, which is always stable for $\omega = 3/5$.

3.2. Third-Order Predictors

The third-order predictors are given by (4) with $m = 3$. We will consider A_1, A_2, and ω as free parameters to reach the best stability. Most of the calculations have been done numerically because the order of the characteristic equation for $A_2 \neq 0$ is five. The following formulas give first the simplest 3-value predictor, followed by optimized 4- and 5-value predictors. The respective ranges of stability are given for $\omega = 1$, the ranges for different ω

can be calculated by (15).

$$A_1 = 0 \qquad A_2 = 0 \qquad \lambda \in (-1/7, 1/2) \tag{21}$$

$$A_1 = -3/5 \quad A_2 = 0 \qquad \lambda \in (-5/11, 5/9) \tag{22}$$

$$A_1 = -1.06 \quad A_2 = -1/3 \quad \lambda \in (-0.842, 0.583) \tag{23}$$

It is seen that the third-order predictors do not cover the whole required range of $|\lambda| < 1$ so that they may be recommended only if it can be guaranteed that the self-consistent field equation is sufficiently fast converging.

The large time-irreversible error term of these predictors (see (11)) must be taken into account as well. The third-order predictors may be eventually combined with the 3-value Gear method for the 2nd order equation with the corrector coefficient $C_0 = 1/6$ which has local error lower than the $C_0 = 0$ method [9] but is not time reversible. The resulting large energy drift is generally considered as disadvantage in molecular dynamics simulations. It can be easily corrected by a friction velocity-dependent term, but a question remains, which method gives better trajectories from the point of view of statistical mechanics.

3.3. Fourth-Order Predictors

The region of stability of fourth-order predictors is very narrow and their applicability is thus limited. For completeness we give here several numerically optimized predictors for $k \leqslant 3$ with their respective ranges of stability for $\omega = 1$:

$$A_1 = 0 \qquad A_2 = 0 \qquad A_3 = 0 \qquad \lambda \in (-1/15, 1/5) \tag{24}$$

$$A_1 = -2/3 \quad A_2 = 0 \qquad A_3 = 0 \qquad \lambda \in (-3/13, 1/4) \tag{25}$$

$$A_1 = -1.29 \quad A_2 = -0.5 \quad A_3 = 0 \qquad \lambda \in (-0.424, 0.281) \tag{26}$$

$$A_1 = -1.85 \quad A_2 = -1.45 \quad A_3 = -0.5 \quad \lambda \in (-0.526, 0.301) \tag{27}$$

Note also that the coefficient at the error term h^4 (see (11)) rapidly grows with increasing k. The time-irreversible error is of order h^5, *i.e.* the same as for the second order predictor with $A_1 = 1/2$, and cannot be improved without substantial loss of stability (the h^5 error term cancels for $k = 1$ and $A_1 = 2/3$ which shrinks the stability range to $\lambda \in (-3/77, 3/28)$).

4. NUMERICAL EXAMPLE

To carry out numerical tests we have chosen liquid acetone simulated recently both with and without polarizability [12]. The model description, simulation details and thermodynamic results not relevant for the present study are given in the Appendix.

4.1. Methodology

The quality of generated trajectories can be monitored by several means. One of them could be the accuracy of the self-consistent field defined by:

$$\delta D^* = \left\langle \max_{i=1}^{n} |\mathbf{D}_i - \mathbf{D}_i^*| \right\rangle / \mu_{\text{acetone}} \tag{28}$$

where the maximum is taken over all molecules in the configuration, μ_{acetone} is the permanent dipole of the acetone molecule (so that δD^* is dimensionless), $\langle \cdot \rangle$ denotes ensemble average approximated by the simulation time average, $\mathbf{D}_i$ denotes the corrector (6), and $\mathbf{D}_i^*$ is the accurate (converged) self-consistent value of induced dipole. (Using a maximum in the above formula instead the standard deviation of $\mathbf{D}_i - \mathbf{D}_i^*$ over all molecules gives a more relevant measure of quality because convergence and stability problems occur at close contacts of particles any may thus reach high peak values.) It would be, however, computationally expensive to calculate the accurate converged solution in each step. We thus use the difference of the values of induced dipoles before and after one iteration which is readily available in the course of the simulation:

$$\delta D = \left\langle \max_{i=1}^{n} |\mathbf{D}_i' - \mathbf{D}_i^p| \right\rangle / \mu_{\text{acetone}} \tag{29}$$

where $\mathbf{D}^p$ denotes the predicted value and $\mathbf{D}'$ the value after one iteration (before mixing it with the old iteration using (3)). The approximate relation between δD^* and its simplified version δD is

$$\delta D^* \approx \delta D \lambda_\omega / (1 - \lambda) \tag{30}$$

provided that operator F is approximately linear and close to diagonal. In (30), λ_ω is the leading eigenvalue of (3) and λ is given by (15).

Another important quantity assessing the quality of MD simulations is conservation of the total energy. It generally consists of two parts, systematic drift E_{drift} and statistical noise δE, which have been separated by linear regression. The energy conservation in shortest time scales is better described by the one-step error defined by

$$\delta E_1 = \langle [E(t) - E(t+h)]^2 \rangle^{1/2} / \langle E_{\text{kin}} \rangle \tag{31}$$

All energy errors are normalized by the average kinetic energy $\langle E_{\text{kin}} \rangle$.

It should be stressed that the values of thermodynamic averages (potential energy, pressure) are, within available precision, insensitive to the choice of the predictor and integration method unless the simulations are performed under extreme conditions (very long integration step), and cannot be used for assessment of the quality of results.

4.2. Convergence Rates

Table I shows the estimates of the minimum and maximum eigenvalues of operator M obtained by equations (14) and (15) from five different configurations and for two polarizability models, from which model A with more pronounced polarizability effects will be used in the rest of the paper (see the Appendix for the details). At the same time, calculating both extreme eigenvalues for the same configuration with different values of the polarizability shows only very small departure from linearity which means that our point-charge model is a good estimate for the linear point-dipole response. Though we will use $(\min\{\lambda_{\min}\}, \max\{\lambda_{\max}\})$ as the range of eigenvalues for optimizing the predictors, we must be aware of the fact that five configurations is not a representative sample and that the peek values will be worse.

Another consequence of the convergence analysis is verification of equation (30). It appears that δD^* is overestimated by equation (30) by

TABLE I The minimum and maximum eigenvalues of matrix M for two polarizable models of liquid acetone obtained by analyzing five randomly chosen configurations. Columns 2 and 3 contain averages over these 5 configurations, the last two columns extremal values

system	$\langle \lambda_{min} \rangle$	$\langle \lambda_{max} \rangle$	$min\{\lambda_{min}\}$	$max\{\lambda_{max}\}$
A	−0.497(7)	0.394(10)	−0.511(3)	0.427(3)
B	−0.464(2)	0.322(08)	−0.467(5)	0.340(5)

10%–30%, and since the leading eigenvalue varies only marginally during the simulation, the simpler error δD is a satisfactory measure of the quality of the self-consistent field.

4.3. Verlet Integration Method

Table II summarises results of runs with the Verlet integrator and several different predictors. These results are divided into four parts. The first one uses the general, always stable second order predictors given by (18) and (20). No particular knowledge of the simulated system has been used to set parameters of these predictors. The runs in the second part use the estimated range of eigenvalues (see the previous paragraph) to determine the best mixing parameter ω by solving equation (17). The same optimization is performed for the partially stable third-order predictor. The last line contains benchmark result with the 'exact' self-consistent field obtained by iterations with accuracy limit $\delta D < \varepsilon = 10^{-6}$.

In accordance with the theory, the lowest energy drift is observed for predictors with $A_1 = 1/2$; from these, the optimized predictor works slightly better. (The drift is even lower than for the 'exact' benchmark run because energy conservation is very sensitive to any irregularity like different number of iterations and resulting tiny random fluctuations. This is also reflected by worse linearity of the benchmark as seen from the large error of E_{drift}.) Comparison with the results with doubled time-step shows that the drift for

TABLE II Different predictors with the Verlet integration method for system A. m is the order of the predictor (4), ω the mixing iteration parameter, δD the relative error of induced dipoles, δE_1 one-step error of the total energy, E_{drift} systematic energy drift and δE the residual standard deviation obtained by linear regression. The energy terms are reduced by the kinetic energy

m	k	ω	A_1	$\delta D/10^{-4}$	$\delta E_1/10^{-4}$	$E_{drift}/[10^{-4}ps^{-1}]$	$\delta E/10^{-4}$	
2	1	0.75	−1.00	17.61(23)	0.2344(40)	−13.5870(40)	0.818	
2	1	1.00	−0.50	9.75(13)	0.2333(40)	−7.1178(31)	0.634	
2	0	0.67	0.00	10.10(14)	0.1706(31)	−5.3707(25)	0.502	
2	1	0.60	0.50	6.02(08)	0.2130(36)	−0.0668(23)	0.466	
2	1	0.96	−0.50	10.46(13)	0.1910(38)	−7.5933(28)	0.581	
2	1	0.96	−0.50	39.9 (7)	0.782(14)	−52.568(19)	3.864	(a)
2	1	0.77	0.50	4.73(06)	0.2196(35)	−0.0417(23)	0.466	
2	1	0.77	0.50	19.94(25)	0.685(12)	−1.5871(72)	1.476	(a)
3	1	0.92	−0.60	1.58(03)	0.1384(23)	5.9936(20)	0.402	
		exact		<0.01	0.1642(28)	0.135(53)	0.342	

(a) double time step $h = 0.002$ ps

$A_1 = 1/2$ scales as h^5 as predicted by (11). It is surprising that these predictors give also the lowest error of the self-consistent field from all second-order predictors in spite of the fact that the maximum root $|\xi_{max}|$ of the characteristic equation is higher for $A_1 = 1/2$ than for $A_1 = 0$ or $A_1 = -1/2$. This witnesses about the importance of time reversibility.

The third-order predictor gives the best accuracy of the self-consistent field and this leads also to slightly better short-time energy conservation, but not to lower long-time energy drift. This is not surprising because some error terms had to decrease, but it does not make sense to simulate the self-consistent field with precision higher than the trajectories themselves.

To provide deeper insight into optimization of the relaxation parameter ω we show in Table III results of short 1 ps runs started from the same initial configuration for predictor (18) with $A_1 = 1/2$ and different ω. The theory, using the maximum range of λ from Table I, gives the optimum $\omega = 0.765$ and divergence for $\omega > 0.794$ (divergence in MD is detected once the error δD exceeds 0.01). While the divergence limit is predicted surprisingly well, no clear minimum of errors for the predicted optimum ω is observed (a very flat minimum for E_{drift} is the only exception). Both phenomena can be explained by considering the time development of matrix M: Extreme eigenvalues of M occur at close contact of polarizable atoms. Such process lasts only a few timesteps, the eigenvalues thus fluctuate and, which is even more important, the corresponding eigenvectors fluctuate fast in time. The predictor is able to survive some instability if it lasts for a short time. On the other hand, the above mentioned λ_{min} and λ_{max} are evidently underestimated and the peak values cause for certain ω an instability which cannot be further stabilized. Both phenomena probably fortuitously cancel out for the estimate of the divergence limit and cause also the lack of apparent optimum; the performance improves with increasing ω (the higher ω, the better estimate of the self-consistent field) until a peek instability occurs.

TABLE III Performance of the second-order predictor with $A_1 = 1/2$ and different values of ω. See Table II for the explanation of the symbols

ω	$\delta D/10^{-4}$	$\delta E_1/10^{-4}$	$E_{drift}/[10^{-4}ps^{-1}]$	$\delta E/10^{-4}$
0.75	4.42	0.1417	−0.1709	0.3439
0.76	4.36	0.1415	−0.1708	0.3429
0.77	4.30	0.1414	−0.1709	0.3420
0.78	4.24	0.1412	−0.1711	0.3411
0.79	4.19	0.1410	−0.1722	0.3402
0.80	unstable			

4.4. Higher-Order Methods

Table IV is a counterpart of Table II for the four-value Gear predictor-corrector integration method. It follows from comparison of these two tables as well as from the run with the exact self-consistent field that a fourth-order predictor would be required to reach the full fourth-order accuracy. Unfortunately, none of the proposed fourth-order predictors is sufficiently stable.

If higher-order methods with low stability are to be used, it is generally necessary to calculate the field more than once in each integration step. It is still possible to use a predictor to have a good guess of the field. The iterations will be controlled by the desired accuracy limit [1] and the necessary number of iterations will be a function of this limit.

This is illustrated in Figure 3 where the number of iterations per step (obtained by short 0.25 ps runs with $\omega = 0.95$ optimized by (16)) is plotted *vs.* the accuracy for the simplest fourth-order predictor and two third-order predictors. All curves have the same overall behaviour: They fall from large values for high accuracies (where the accuracy of the predictor is much lower than the required accuracy) until they reach certain point (where the accuracies are balanced) and remain constant for lower accuracies. This limit is 1 for the third-order predictor (22) because it is stable for our system but as high as 2 for the fourth-order predictor; also this value is predicted by the theory because the maximum eigenvalue of $[\omega M + (1-\omega)]^2$ for $\omega = 0.95$ falls into the stability limit (24).

It is interesting that the error bar for $\varepsilon = 10^{-5}$ is zero, *i.e.* exactly 2 iterations were required in each step. Accuracy 10^{-5} is thus the optimum accuracy for the fourth-order predictor in our simulation. Compared to the

TABLE IV Different predictors with the four-value Gear predictor-corrector method. See Table II for the explanation of the symbols

m	k	ω	A_1	$\delta D/10^{-4}$	$\delta E_1/10^{-4}$	$E_{drift}/[10^{-4}ps^{-1}]$	$\delta E/10^{-4}$	
2	1	0.96	−0.50	10.32(13)	0.1254(23)	−7.4256(21)	0.436	
2	1	0.77	0.50	4.59(05)	0.0953(17)	−0.2436(12)	0.238	
2	1	0.77	0.50	19.39(46)	0.665(11)	−34.460(7)	1.422	(a)
3	1	0.92	−0.60	1.64(03)	0.0794(12)	6.1381(14)	0.278	
3	1	0.92	−0.60	12.31(22)	0.652(10)	9.062(12)	2.403	(a)
3	2	1.00	−1.06	2.22(03)	0.0770(11)	7.8495(13)	0.259	(b)
		exact		<0.01	0.0650(10)	−0.146(16)	0.105	

(a) double time step $h = 0.002$ ps
(b) $A_2 = -1/3$

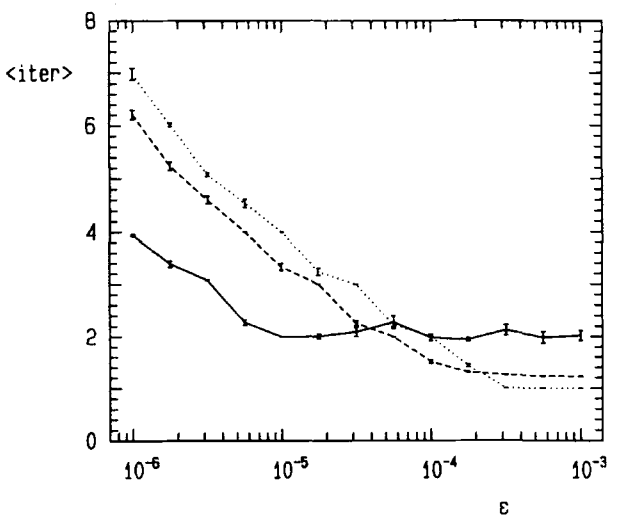

FIGURE 3 Number of self-consistent field iterations per integration step as the function of accuracy limit ε for liquid acetone simulated by the four-order Gear predictor-corrector integration method. Solid line: fourth-order predictor (24); dashed line: third-order predictor (21); dotted line: third-order predictor (22).

Verlet simulations, we have to pay 50% efficiency for the fourth-order accuracy.

Using lower precision of the self-consistent field or a lower-order predictor with higher order integrator is generally a bad idea (unless the polarizability effects represent a small perturbation only) – if lower accuracy is sufficient, the integration step may be increased to have the errors of different parts comparable.

5. CONCLUSIONS

This work shows that molecular dynamics simulations with the electrostatic interactions including polarizability effects do not require expensive iterations to obtain the self-consistent field provided that the values of this field are predicted from previous step.

The overall best results have been obtained with the Verlet integration method and self-consistent field predictor given by (18) with parameter $A_1 = 1/2$. If the relaxation parameter (see (3)) is $\omega = 0.6$, the method is stable for all physically stable systems and may be used in practice, though know-

ledge of convergence properties of the equation for the self-consistent field may help to improve performance.

We have not found any always stable higher-order predictor. Partial stability of these predictors suitable for higher-order integration methods means that they may be used either if the convergence of the equation for the self-consistent field is sufficiently fast or if more iterations per integration step are performed.

Acknowledgements

This work was supported by the DOE-LPB electrochemical storage program and the Danish Research Council's special programme in Information Technology. Helpful discussions with Prof. E. R. Smith (Latrobe University, Australia) and Prof. I. Nezbeda (Academy of Sciences, Prague) are greatly acknowledged.

APPENDIX: SIMULATION DETAILS

The testing system is a four-site model of liquid acetone $CH_3CO\,CH_3$ taken from [12] with minor changes.

United atom representation is adopted for groups CH_3 so that the acetone molecule is described by four interaction sites. The intermolecular site-site interactions consist of Lennard-Jones terms and Coulomb interactions. While the molecule in [12] is rigid, we allow the bond angles bend and add improper torsion [13] to keep the molecule planar. These additional energy terms are taken from [14]. Bond lengths are constrained.

The polarizability is modelled by auxiliary charges [4]. Charge Ne, where N is the number of outer shell electrons, is added to the polarizable site (which already has some partial charge). The additional charge is compensated by negative charge $-Ne$ whose position $\mathbf{r}$ relative to the site is derived from the electrostatic force $\mathbf{F}$ acting on it:

$$\mathbf{r} = \frac{\alpha}{N^2 e^2}\mathbf{F} \tag{32}$$

where α is the polarizability. Our estimate of the number of necessary operations suggests that this approach is computationally more efficient than modelling polarizability by point dipoles added to partial charges at the same site.

Most of the presented results have been obtained by the simplest possible model (model A) in which only one atom, namely the central carbon atom, bears the whole polarizability, $\alpha = 6.42$ Å^3 [12]. We have chosen $N = 24$ as the number of all valence electrons in the acetone molecule. For comparison we include also some results for (probably more realistic) model B with all atoms polarizable; the polarizability is in this case distributed according to the number of valence electrons ($N_C = 4, \alpha_C = 104$ Å^3; $N_O = 6, \alpha_O = 1.56$ Å^3; $N_{CH_3} = 7, \alpha_{CH_3} = 1.82$ Å^3).

The cubic simulation box contains 256 acetone molecules in the usual periodic boundary conditions and density 789.9 kg/m^{-3}. To treat the electrostatic interactions accurately, the Ewald summation is used. The set of Ewald parameters ($\alpha_{\text{Ewald}} = 0.21142$/Å, $K = 6.53875$, real-space cutoff radius = one half of the box size) follows from the error estimates published in [15] for the expected errors of forces acting on the maximum charge set to $0.05k_B$K/Å in real-space and $0.2k_B$K/Å in the reciprocal space, where k_B is the Boltzmann constant. These estimates were calculated for the original system (without the auxiliary charges). (This is enabled by the structure of our algorithm for the real-space Ewald sum which first calculates the site-site distance, and when this distance is less than the real-space cutoff, all electrostatic interactions between these two sites including the auxiliary charges are evaluated even if the distance of the auxiliary charges is larger than the cutoff.)

The bond lengths are constrained either by SHAKE [9] for the Verlet integrator, or by calculating the constraint forces via the Lagrangian multipliers [9, 16] for the Gear predictor-corrector integrator for the second order equation. Unnecessarily high precision calculations are performed in both cases to avoid any uncontrolled sources of errors.

Most of the simulations were carried out in the standard microcanonical ensemble with the time step $h = 0.001$ ps and temperature fluctuating around $T = 300$ K. The productive runs lasted 10 ps and started from configurations taken from previous runs which were further equilibrated within 1 ps with friction thermostat ($T = 300$ K, relaxation time 0.25 ps).

Selected thermodynamic results are compared in Table V with the results of [12]. Our results were obtained by 10 ps runs and separate friction thermostats ($T = 25$°C) for inter-and intramolecular motions to overcome their weak coupling. For systems A and B the Verlet method with the optimum predictor ($m = 2, k = 1, A_1 = 0.5, \omega = 0.77$) was used, the NP result is an average from essentially identical Gear and Verlet runs. Small differences between our and literature results can be attributed to the differences of the models. The polarizability effects described by $\langle|\mathbf{D}_i|\rangle$ are most

TABLE V Thermodynamic results for the testing system of liquid acetone at $T = 25°C$. NP denotes the nonpolar system, A the system with the central carbon polar, B the system with all atoms polar. U is the averaged potential energy without bond-angle and torsion terms, $\mathbf{D}_i$ the effective (permanent + induced) dipole moment of one acetone molecule and P is pressure

system	$U/[kJ\ mol^{-1}]$	$\langle\|\mathbf{D}_i\|\rangle/\mu_{acetone}$	P/MPa
NP	−29.44(04)	1	66(3)
NP[12]	−29.07(15)	1	
A	−32.70(05)	1.221(2)	53(3)
A[12]	−31.72(27)	1.198(10)	
B	−31.85(04)	1.162(1)	58(3)

pronounced for model A with one polarizable atom and flexible molecule. If the molecule is rigid then the polarizable atoms cannot approach each other so easily which is probable explanation of slightly lower value of $\langle|\mathbf{D}_i|\rangle$ reported in [12]. The lowest polarizability effects are observed for model B with distributed polarizability.

References

[1] Vesely, F. J. (1977) "N-particle dynamics of polarizable Stockmayer-type molecules", *J. Comput. Phys.*, **24**, 361.

[2] Pollock, E. L., Alder, B. J. and Patey, G. N. (1981) "Static dielectric properties of polarizable Stockmayer fluid", *Physica*, **108A**, 14.

[3] Van Belle, D., Couplet, I., Prevost, M. and Wodak, S. J. (1987) "Calculations of electrostatic properties in proteins. Analysis of contributions from induced protein dipoles", *J. Mol. Biol.*, **198**, 721.

[4] Zhu, S.-B., Yao, S., Zhu, J.-B., Surjit Singh and Robinson, G. W. (1991) "A flexible/polarizable simple charge water model", *J. Phys. Chem.*, **95**, 6211.

[5] Ahlström, P., Wallqvist, A., Engström, S. and Jönsson, B. (1989) "A molecular dynamics study of polarizable water", *Mol. Phys.*, **68**, 563.

[6] Ruocco, G. and Sampoli, M. (1994) "Computer simulation of polarizable fluids: a consistent and fast way for dealing with polarizability and hyperpolarizability", *Mol. Phys.*, **82**, 875.

[7] Sprik, M. and Klein, M. L. (1988) "A polarizable model for water using distributed charge sites", *J. Chem. Phys.*, **89**, 7556.

[8] Sprik, M. (1991) "Computer simulation of the dynamics of induced polarization fluctuations in water", *J. Phys. Chem.*, **95**, 2283.

[9] Allen, M. P. and Tildesley, D. J. *Computer Simulations of Liquids* (Clarendon Press.) (1987).

[10] Gear, C. W. *Numerical Initial Values Problems in Ordinary Differential Equations* (Prentice Hall) (1971).

[11] Ralston, A. *A First Course in Numerical Analysis* (McGraw-Hill) (1965).

[12] Jedlovszky, P. and Pálinkás, G. (1995) "Monte Carlo simulation of liquid acetone with a polarizable molecular model", *Mol. Phys.*, **84**, 217.

[13] Brooks, B. R., Bruccoleri, R. E., Olafson, B. D., States, D. J., Swaminathan, S. and Karplus, M. (1983) "CHARMM: A Program for Macromolecular Energy, Minimization, and Dynamics Calculations", *J. Comput. Chem.*, **4**, 187.

[14] QUANTA Parameter Handbook (Polygen Corporation) (1990).
[15] Kolafa, J. and Perram, J. W. (1992) "Cutoff errors in the Ewald summation formulae for point charge systems", *Molec. Simul.*, **9**, 351.
[16] de Leeuw, S. W., Perram, J. W. and Petersen, H. G. (1990) "Hamilton's equations for constrained dynamical systems", *J. Stat. Phys.*, **61**, 1203.